한국소음진동공학회 2000년도 추계학술대회논문집, pp. 790~795.

디스크 플러터에 기인한 헤드위치 오차와 허용 트랙밀도의 추정

°박대경*, 장영배*, 박영필**

Head Positioning Error due to Disk Flutter and Estimation of Permissible Track Density

°Dae-Kyong Park*, Young-Bae Chang*, and Young-Pil Park**

Abstract

디스크마다 일정영역을 할당하여 위치정보를 기록하는 임베디드 서보방식 하드디스크는 데이터가 저장되는 데이터 영역사이에서 스핀들 런아웃, 공진과 디스크 플러터 등에 의하여 Gaussian 분포를 가지는 트랙에서 벗어나는 오차를 가지게 된다. 더높은 저장밀도와 빠른 기록속도를 요구함에 따라서 디스크의 회전속도가 올라감에 의한 디스크 면진동에 의한 헤드 위치오차가 중요하게 대두되고 있다. 본 연구에서는 헤드위치 오차량을 계산하기 위하여 고속탐색이 가능한 수정된 Barasch의 수치해석법, 유한요소법, 그리고 실험을 통하여 적용가능성을 확인하였으며 같은 드라이브내에서 디스크의 사이즈를 바꿈에 의한 디스크 동특성의 해석과 변환율을 이용하여 오류가 발생할 수 있는 트랙 벗어남과 저장밀도의 상관관계를 살펴보았다.

I. Introduction

Demand for higher data storage capacity in hard disk drives makes to grow exponentially at a very aggressive rate in areal density of hard-disk drives. Increase of a high track density for a high areal density has led to ever shortening the width of track. And the increase of a rotating speed for a high transfer rate and access time is one of the major sources of track misregistration which is caused by various run-outs, such as disk vibration, spindle disturbance and air turbulence in disk drive. In the embedded servo which is used in most HDD servo systems at present, information of servo sector is written in disk at regular intervals. The servo burst field has the information that how much the R/W head is offset from the target track center. But compensation of track misregistration using signal of burst signals makes it difficult to predict the off-track quantity to next servo sector. Therefore we have difficulty in estimating behavior of head in data region when the head reaches to next

* Yonsei Univ. Graduate Student
** Yonsei Univ. Professor

servo sector. If track misregistration is over the limits of desirable quantity, the head makes it a mistake to read/write in desired track.

Disk runout consists of repeatable runout (RRO) which is repeated at each revolution and non-repeatable runout (NRRO) which is not repeated at each revolution. Because most of RRO can be compensated by tracking servo control, NRRO is the main cause of track misregistration which prevents a high track density.

II. Theoretical Background

2.1.Vibration characteristic of rotating disk

Disk vibration is an important contributor to track misregistration. Though hard disk has met the TMR requirement, in the present day the demand of much higher TPI impels to understand the accurate information of the hard disk slider system.

The vibration characteristics of rotating disk varies by regular rule in accordance with rotating speed. And if the rotating speed reaches to critical speed, the very small external force gives rise to perform the large deflection and performance and stability of hard disk system go down. Contrary to stationary disk, the rotating disk vibration problem contains simultaneously the vibration phenomenon of circular disk and membrane. The vibration phenomenon of membrane happens because centrifugal force generates tension in infinitesimal element and the effect of membrane vibration is superior to that of circular disk vibration because the faster rotating speed is, the larger centrifugal force. The problem of disk vibration is induced from the equilibrium of all transverse force and inertia force which operates on infinitesimal element with infinitesimal displacement. The shear force which acts as transverse force is arranged for the moments using the equation of moment equilibrium that is derived from the infinitesimal element and in the next place the moment is arranged by the partial differentiable value of transverse displacement using the curvature. At last, the shear force is eliminated, and the problem is arranged as the partial differentiable equation of transverse displacement. And the vibration problem of membrane is induced from the equilibrium of transverse force and inertia force when the infinite displacement happens in the infinitesimal element which is suppressed by the tension. The figure 1 shows that the vibration characteristic that is represented by nodal circle and nodal diameter is expressed as the change of natural frequency according to the rotating speed. The mode splitting as to rotation associated with the resulting forward and backward traveling wave frequencies with respect to the stationary mode which is expressed by each one mode.[1]

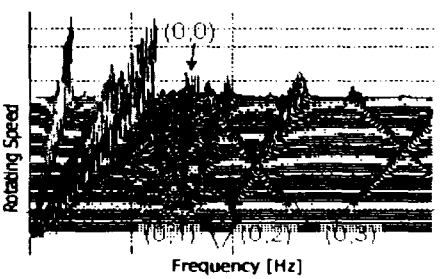

Figure 1. The natural frequencies of out-plane vibration of circular disk according to the rotating speed

2.2. Disk flutter and vibration characteristic of slider.

The figure 2 shows the spectrum of the axial vibration velocity that is measured by the Laser Doppler Vibrometer (LDV). The spectrum is measured in constant rotating speed.

In figure 2, the modes ,such as (0,0), (0,1), (0,2) mode, are shown as forward and backward modes. The narrow peaks is rocking mode by spindle bearing and repeatable runout. Whereas wide peaks are components of flutter by rotating disk.

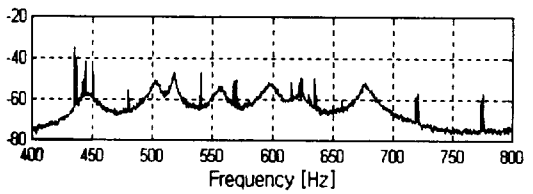

Figure 2. The spectrum of the axial disk vibration at outer region of disk

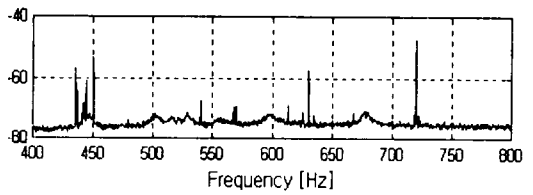

Figure 3. The spectrum of the radial slider vibration at outer region of disk

The spectrum of slider vibration velocity in track direction is shown in figure 3. The slider is located at the same track where the disk vibration is measured in figure 2 and travels continuously. Investigating the vibration characteristics of figure 2, 3, we find out that the peaks in figure 2 correspond to the peaks in figure 3. This means that there is interrelation between disk vibration and slider vibration.

2.3. Head off-track mechanism by disk flutter.

Assuming that the slider's roll center locates at the top of slider and the flutter exiting force is a constant load which is distributed over the disk. Then the total head off-track dx by disk flutter is[2],

$$\triangle x = (t_s + t_d/2) \cdot \theta \qquad (1)$$

where Both t_s and t_d are the thickness of slider and disk. And θ is disk inclination angle.

And we are able to express that the disk deflection and disk inclination angle are function of radius (r). By these disk deflection, disk inclination angle and thickness of both disk and slider, we define the transfer ratio as following equation.

$$k = (t_s + t_d/2) \cdot \frac{\theta(r)}{v(r)} \qquad (2)$$

from those equations, head off-track dx in equation(1) is

$$\triangle x = k \times v(r) \qquad (3)$$

III. Calculating the transfer ratio.

3.1. Numerical Method : Reformed Barasch Method

Figure 5, 6 illustrate stress, shear force, and moment that act upon the infinitesimal element of rotating disk. If we assume that the thickness is very thin, we are able to assume the plane stress state. Because tensile stress by centrifugal force is applicable to the tension in problem of string vibration, we can induce the term about stress. Substituting six transverse forces which act upon infinitesimal element by tensile force and shear force, we are able to express the conventional modeling of rotating disk.[1]

$$\begin{aligned}\rho h \frac{\partial^2 w}{\partial t^2} &= \frac{\partial}{r\partial r}(Q_r r) + \frac{\partial}{r\partial\theta}(Q_\theta) \\ &+ \frac{\partial}{r\partial r}(\sigma_r h r \frac{\partial w}{\partial r}) + \frac{\partial}{r\partial\theta}(\sigma_\theta h \frac{\partial w}{r\partial\theta}) \\ &+ \frac{\partial}{r\partial\theta}(\sigma_{r\theta} h \frac{\partial w}{\partial r}) + \frac{\partial}{r\partial r}(\sigma_{r\theta} h r \frac{\partial w}{r\partial\theta}) \\ &+ q_w(r, \theta, t)\end{aligned} \qquad (4)$$

If we perform the modal analysis using stress analysis after eliminating the shear force by moment equilibrium, we obtain following 4th order differential equation.

$$L[w] + M\ddot{w} = f_w \qquad (5)$$

where

$$L[w] = D\nabla^4 w - H[w]$$

$$H[w] = \frac{h}{r}\frac{\partial}{\partial r}\left(\sigma_r r \frac{\partial w}{\partial r}\right) + \frac{h}{r^2}\sigma_\theta\left(\frac{\partial^2 w}{\partial\theta^2}\right)$$

$$\sigma_r = A\rho\Omega^2\frac{1}{r^2} + 2B\rho\Omega^2 - \frac{3+\nu}{8}\rho\Omega^2 r^2$$

$$\sigma_\theta = -A\rho\Omega^2\frac{1}{r^2} + 2B\rho\Omega^2 - \frac{1+3\nu}{8}\rho\Omega^2 r^2$$

$$A = \frac{(1-\nu)[(3+\nu)a^2 - (1+\nu)b^2]a^2b^2}{8[(a^2+b^2)+\nu(a^2-b^2)]}$$

$$B = \frac{(1+\nu)[(3+\nu)a^4 + (1-\nu)b^4]}{16[(a^2+b^2)+\nu(a^2-b^2)]}$$

S.Barasch and Y.Chen solved equation simultaneously by assuming arbitrary natural frequency and arbitrary initial problem and substituted 4 first order differential equations for 4th order differential equation. Therefore, we only decide that the function R(r) of radial direction meets all boundary conditions because the function R(r) subjects to governing equation automatically. Until we obtain the solution of R(r) which satisfies the boundary condition, we iterate the natural frequency . Let

$$x = \{R_1, R_2, R_3, R_4\}^T \quad (6)$$

$$R_1 = R,\ R_2 = R',\ R_3 = R'',\ R_4 = R'''$$

which leads to a system of 4 first order differential equations. We get the displacement and angle of disk flutter using these procedure outlined by Barasch and Chen. In particular, when we calculated natural frequencies in rotating coordinate, an estimation procedure using a cantilever and conic curves was considered. It accelerated the convergence speed of Barasch's method and computational sensitivity analysis could be done.

3.2. FEM

Following figures are the mode shapes about stationary disk. We can calculate the ratio of disk displacement and tilting angle using FEM. We used the Nastran program.

(a) (0,0) Mode (b) (0,1) Mode

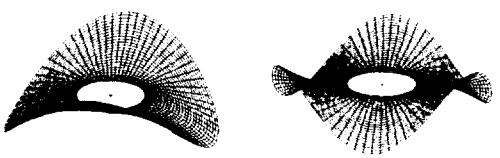

(c) (0,2) Mode (d) (0,3) Mode

Figure 4. Disk Vibration Mode using FEM

3.3. Experiment

3.3.1 Block Diagram of HDD Servo System

Figure 5 shows the simple block diagram of the HDD track-following servo system. As shown in the figure 5, there are four inputs (r, w, d, n) and one output (y) that is true PES, that is, the signals indicating the actual error between the head position and the target track center. These signals are made up through the various equipments and processes. Particularly, d represents mechanical output disturbance and includes spindle motor/ball bearing vibration, disk vibration due to the high-speed spindle rotation and imperfections in the servo-written track circle.

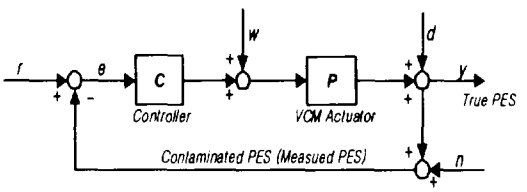

Figure 5. Block Diagram of HDD track following servo system

The servo burst field that has the information about head positioning error compensates for TMR by runout in HDD. As shown in Figure 5, output $y(t)$ can be expressed as follows.

$$\begin{aligned} PES(k) = & \frac{P(z)}{1+P(z)C(z)}\,w(k) \\ & + \frac{1}{1+P(z)C(z)}\,d(k) \\ & + \frac{1}{1+P(z)C(z)}\,n(k) \qquad (7) \\ = & \ S(z)\{P(z)w(k)+d(k)+n(k)\} \end{aligned}$$

From Eq. (2.3), the contaminated PES by mechanical runout used in controller is determined by sensitivity transfer function, only.

3.3.2 Experimental Setup

Figure 6 shows the layout of the mechanical measurement setup. An LDV is used to measure the axial velocity power spectrum of disk and the radial velocity power spectrum of slider to obtain the transfer ratio from equation (3). As we investigated in former section, same vibration characteristics are shown.

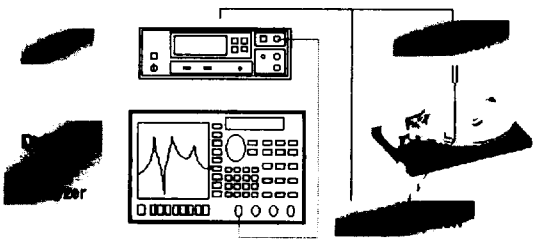

Figure 6. Experimental Setup

Inducing transfer ratio from the equation (3), we measured the spectrum of axial disk vibration and the spectrum of radial slider vibration using LDV. And we performed the measurement from the first track at inner region of disk to the last track at outer region of disk successively. When the head maintains tracking mode at each track, velocity spectrum measurements were measured with a beam passing through a slot in the top case and side case.

Because the off-track amount is actual head displacement due to disk flutter, the result that controlled by closed-loop error signal is compensated using the gain of the sensitivity transfer function.

3.4. Result

The average result that is the position error amount from three methods was summarized in table 1. We affirmed the application possibility that the transfer ratio that is calculated using both the reformed numerical method and FEM method is the same with the result for experimental method.

Table 1. Transfer Ratio

	Average of Transfer Ratio		
	Numerical Method	FEM	Experimental
Outer (r=45mm)	1 / 28.4	1 / 28.7	1 / 27.6
Middle (r=33mm)	1 / 14.1	1 / 14.3	1 / 15.1
Inner (r=20mm)	1 / 2.6	1 / 2.8	1 / 4.7

IV. Admissible off-track amount due to disk flutter about approximate track density.

4.1. Limit of Flutter Amplitude

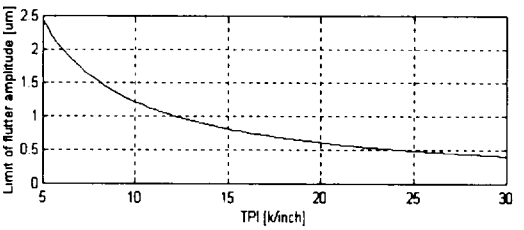

Figure 7. Limit of flutter margin of head positioning error

We estimated the off-track amount due to disk flutter as to approximate track density. In practice, head position error occurs if the misregistration is greater than approximately 12 percents of the track width. And if we consider that what percents are the components of disk flutter, we are able to estimate the head positioning error by disk flutter according to TPI that we want to design. Considering the misregistration by transfer ratio and servo sensitivity function gain, it is possible that we predict the quantity of disk flutter by the disk vibration characteristic ,except disk static deformation and RRO components, according to TPI.

Disk flutter is calculated by the method of 3 σ TMR. And the calculation is iterated according to rotating speed and disk size.

Table 2. Disk Vibration Amplitude by 3σ TMR

	Total Vibration	Flutter Vibration
5400 rpm	1.6850 ㎛	0.7989 ㎛
7200 rpm	2.8261 ㎛	1.1487 ㎛
10000 rpm	4.7257 ㎛	1.4836 ㎛

4.2. Vibration Characteristics of Alternate Disk Size

When disk size is changed by reformed numerical method, we researched the change of

vibration characteristic. Table 3 shows both natural frequency and the reciprocal of transfer ratio when disk diameter is altered.

Table 3. Natural Frequencies and Transfer Ratio of Alternate Disk Size

Diameter	Natural Frequency [Hz]			Average 1/transfer ratio
	(0,0)	(0,1)	(0,2)	
3 in	1208.8	1221.6	1404.2	20.77
3.5in	748.68	748.64	886.45	26.79
4in	517.62	513.06	625.15	33.21

4.3. Disk Flutter of Alternate Disk Size

First, in alternate disk radius, the ratio between the value of transfer ratio at each mode and the flutter amount is normalized on the basis of 3.75in disk. And later we calculate the admissible head positioning error due to disk flutter by multiplying the measured axial disk vibration amplitude.

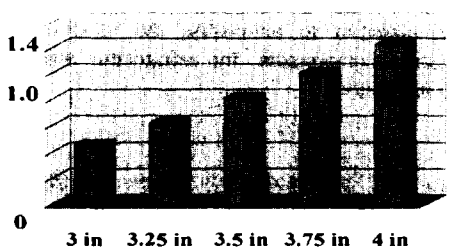

Figure 8. Normalized Disk Vibration

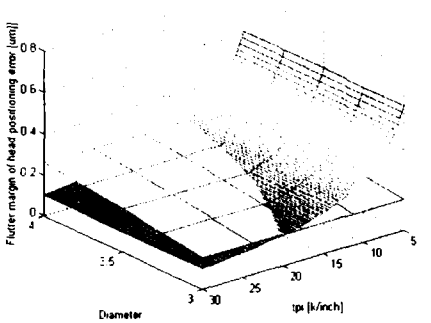

Figure 9. Flutter margin of head positioning error at 7200 rpm in case of alternate radius

V. Conclusion

Investigating the head positioning error, we researched the numerical method by using a cantilever and conic curves and FEM method with Nastran and verified the suitability of transfer ratio's assumption through the experiment. Besides, the method that makes prediction of the track density possible is presented when the change of disk flutter and transfer ratio is considered in another disk size.

Acknowledgement

This work was funded by the Korea Science and Engineering Foundation (KOSEF) through the Center for Information Storage Device (CISD) Grant No. 2000G0101

References

(1) E.G.Lim, Master courese paper, "Natural Frequency analysis of a Rotating Circular Disk in Information Storage Devices",1999

(2) Satomitsu I. and Toshihisa O., "Flutter Reduction by Centrifugal Airflow for High-Rotating-Speed Disks" Adv. Info. Storage Syst. Vol.9, 1998

(3) Padmanabhan S. and Kumar K. "Prediction TMR from disk vibration of alternate substrate materials", IEEE Transactions on Magnetics, Vol.36, 2000